

Generic features of the phase transition in cold and dense quark matter

Kenji Fukushima

Department of Physics, Keio University, Kanagawa 223-8522, Japan

We investigate the phase transition in cold and dense quark matter in an intuitive way that shares common features of the effective model approaches. We first express the quasi-particle contribution to the thermodynamic potential with the dynamical mass M and then discuss how we can understand the possible first-order phase transition with and without the vector interaction from the saturation curve on the plane of the energy per particle and the density. We next extend our analysis including inhomogeneity and discuss the relation between the order of the phase transition and the saturation curve. We emphasize that the saturation curve is useful to infer qualitative nature of the phase transition even without knowing the explicit solution.

PACS numbers: 21.65.Qr, 12.38.Mh, 25.75.Nq

The quest for the phase diagram of strongly interacting matter out of quarks and gluons (i.e. matter described by Quantum Chromodynamics – QCD) is one of the most challenging problems in modern theoretical and experimental physics. There are many speculations on the QCD phase diagram from theory such as the color-superconducting phase [1], the quarkyonic state [2] and the triple-point-like structure [3], the QCD critical point [4], and so on (see Refs. [5, 6] for reviews). Available experimental information [7] is, however, too limited to constrain uncertainties on those speculative possibilities (see Ref. [8] for an attempt and also Refs. [9, 10] for interpretations). Among others, the QCD critical point search is vigorously ongoing in the present and future experimental facilities as well as in the first-principle calculation of the lattice-QCD simulation.

The QCD critical point would be, if discovered, a landmark for our understanding on QCD matter. In an infinite-volume system at equilibrium, the fluctuations are expected to show critical behavior and thus the criticality serve as experimental signatures [11]. There are many theoretical proposals and experimental data taken from the beam-energy scan program at Relativistic Heavy Ion Collider (RHIC) in the Brookhaven National Laboratory. It is an urgent question to make clear whether the QCD critical point exists and, if any, where it is located.

Because of the notorious sign problem with finite quark chemical potential μ_q , the importance sampling breaks down in finite-density simulations. Although theoretical attempts are making steady progresses, (temporal) finite-volume effects are not easily treatable [12], and it is still difficult to extract any reliable conclusion even on a qualitative level. Then, under these circumstances, there are three major passages toward the QCD phase diagram studies (except for recent developments in the functional method [13]),

1. One can discuss the critical phenomena *assuming* the QCD critical point. This is a common strategy of theory in general. Since the critical properties are universal, one can make model-independent predictions. The virtue of this approach is the generality, but it does not give any clue about the existence and/or the location of

the critical point.

2. One can utilize the effective model description with a reasonable choice of the model parameters [14]. The location of the critical point is sensitive to model details. Not that all model results are model dependent, but the nature of the phase transition at high density strongly depends on a part of the model setup, as we will elucidate later.

3. One can make a conjecture on the phase structure based on generic properties of QCD such as symmetries [15, 16] and the degrees of freedom in a particular limit [2]. Because the argument lacks for concrete dynamics unlike the model study, one should check individually which scenario is favorable in reality. Nevertheless, such a conjecture from physics deliberation provides us with a useful guideline for model analysis.

The aim of the present work is to establish a path from 2 to 3 in the above classification. This is a route rather opposite to conventional approaches. Instead of choosing a particular model description, we shall extract the essential ingredients common in most model studies and try to unveil underlying physics mechanism in a way free from model artifacts. In particular, by looking at the saturation curve, i.e. the energy per particle as a function of density, we can clearly see the nature of the liquid-gas phase transition, which also enables us to understand why the vector interaction would disfavor the first-order phase transition. It is a straightforward extension to include inhomogeneity as the chiral spiral for simplicity, and we can then find that the phase structure still has rich contents, which is again understandable from the saturation curve.

Let us start our analysis utilizing the same setup as Ref. [17]. We treat cold and dense quark matter in a quasi-particle description. (This means that we assume a Fermi liquid of quark matter, which should be valid for bulk thermodynamic quantities as long as T is small enough and the Landau damping is a minor effect.) In this way the thermodynamic potential from quasi-particles, Ω_{matter} , is expressed as a function of the

effective mass M in a form of

$$\begin{aligned} \Omega_{\text{matter}}[M]/V = & - \int_0^{\mu_q} d\mu' \rho(\mu') \\ & - 4N_c N_f T \int \frac{d^3 p}{(2\pi)^3} \ln(1 + e^{-\omega_p/T}), \end{aligned} \quad (1)$$

where $\rho(\mu)$ is the quark number density defined by $\rho(\mu) = 2N_c N_f \int \frac{d^3 p}{(2\pi)^3} [n_F(\omega_p - \mu') - n_F(\omega_p + \mu')]$ with the Fermi-Dirac distribution function, $n_F(\omega_p) = (e^{\omega_p/T} + 1)^{-1}$, and the quasi-particle energy, $\omega_p = \sqrt{p^2 + M^2}$. It is important to note that this μ_q -dependent matter part is common in any quark models such as the (P)NJL model and the (P)QM model [14]. Then, the model uncertainty is unavoidable in the vacuum part.

In a quasi-particle picture of quarks the vacuum part could be expressed as $\Omega_0[M]/V = -2N_c N_f \int^\Lambda \frac{d^3 p}{(2\pi)^3} \omega_p + U[M]$ with a potential term. If we postulate it as $U[M] = (M - m)^2/(4g_s)$, then $\Omega_0[M] + \Omega_{\text{matter}}[M]$ exactly amounts to the thermodynamic potential in the NJL model with the bare mass m [18]. To implement the $U(1)_A$ anomaly in the three-flavor case, we may add a term $-g_d(M - m)^3$ in $U[M]$. From now on, we shall adopt a more general form of $\Omega_0[M]$ inspired by the Ginzburg-Landau expansion, i.e.

$$\Omega_0[M]/V = a(M_0^2 - M^2)^2 - bM - cM^3. \quad (2)$$

Although the thermodynamic potential in hand is extremely simple, this setup sufficiently grasps the generic features of the phase transition in cold and dense quark matter. To enter the regime at higher temperature, however, one should consider the meson fluctuations that may give rise to T -dependent coefficients in Eq. (2). Therefore, strictly speaking, our analysis is valid only in the region with $\mu_q \gg T$. In what follows we consider only the $c = 0$ case, for we are interested in the mechanism in favor of the first-order phase transition and $c \neq 0$ would trivially stabilize the first-order transition.

Figure 1 shows the typical behavior of the potential. As discussed in Ref. [17] the matter part Ω_{matter} always has a minimum at $M = 0$ because the baryon density is the largest when quasi-particles are massless. Let us consider the condition for the first-order phase transition in the case of $T = 0$ in which Eq. (1) simplifies as: $\Omega_{\text{matter}}/V = -(N_c N_f / 12\pi^2) (p_F \mu^3 - \frac{5}{2} M^2 p_F \mu + \frac{3}{4} M^4 \ln[(\mu + p_F)/(\mu - p_F)]) \theta(\mu - M)$ with $p_F = \sqrt{\mu^2 - M^2}$. In Ref. [17] the upper bound for the curvature a was estimated under a reasonable but limited situation, $\mu_q \simeq M_0$. We can relax this numerically only to find that a first-order phase transition can remain in the chiral limit ($b = 0$) unless μ_q is unphysically larger than M_0 (for which Ω_{matter} stretches far beyond $M \sim M_0$).

This simple analysis tells us that the first-order phase transition at $T = 0$ can occur since Ω_{matter} is proportional to $\theta(\mu - M)$ and Ω does not have to contain a

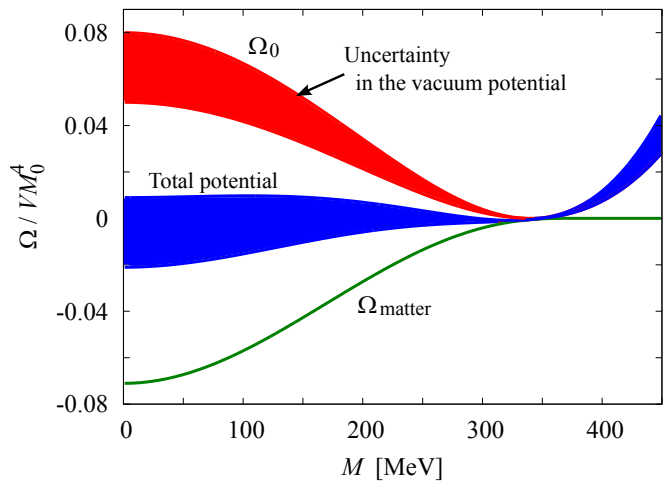


FIG. 1. Potential shapes from Eqs. (1) and (2) at $T = 0$ with $\mu_q = 370$ MeV. Ω_{matter} is model independent, while the vacuum potential Ω_0 leaves uncertainty. The parameters in Ω_0 are chosen as $M_0 = 340$ MeV and the curvature from $a = 0.05$ (\approx a value in the linear σ model) to $a = 0.08$ (\approx a value in the NJL model), and $b = c = 0$.

M^6 term, while Ω is sometimes assumed to take a form of $c_2 M^2 + c_4 M^4 + c_6 M^6$ at $T \neq 0$. Thus, the present formalism based on the quasi-particle approximation is more appropriate for the investigations of cold and dense quark matter.

Furthermore, we must add a term $\propto \rho^2$ in Ω_{matter} , which stems from the vector-channel interaction $(\bar{\psi}\gamma_\mu\psi)^2$ that is chiral symmetric [19], i.e.

$$\Omega_{\text{vec}}[M]/V = g_v \rho^2, \quad (3)$$

which can be evaluated with $\rho = \frac{N_c N_f}{3\pi^2} (\mu^2 - M^2)^{3/2} \theta(\mu - M)$ at $T = 0$. We should note that in the mean-field approximation for the vector interaction, usually, it shifts the chemical potential, which pushes the energy up by $\sim 2g_v \rho^2$, and the condensation energy is negative, $-g_v \rho^2$, leading to $\sim 2g_v \rho^2 - g_v \rho^2 = g_v \rho^2$ in total.

For a deeper insight, Fig. 2 is quite instructive. This figure shows the location of two degenerate minima in the potential (i.e. the dynamical mass) when μ_q takes a value at the first-order phase transition. For example, in the chiral limit, the dynamical quark mass jumps from $M \simeq M_0$ to $M = 0$. The jump is naturally reduced at larger b (larger quark mass) and eventually only crossover remains beyond the bend of the curves in Fig. 2. One can notice that the curve substantially shrinks with positive g_v which disfavors the first-order phase transition.

It is interesting to see that the vector interaction has only a minor impact for $b = 0$. This is because the minimum at $M = 0$ is intact as long as chiral symmetry is exact at $b = 0$ and ρ and thus the vector interaction is still very small at $M = M_0$. Guided by Fig. 2 we shall specifically look at the following three cases: (1) $b = g_v = 0$ (first-order), (2) $b = 0.08M_0^3$ and $g_v = 0$

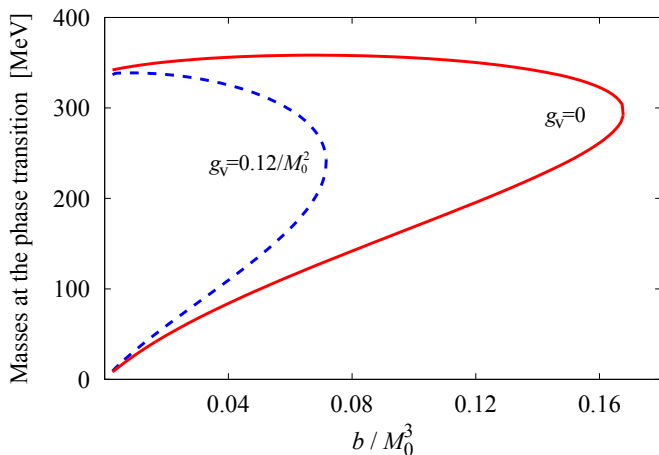


FIG. 2. The location of the potential minima at the first-order transition point when $g_v = 0$ (solid curve) and $g_v = 0.12/M_0^2 \simeq 10^{-6} \text{MeV}^{-2}$ (dashed curve) are chosen, respectively, with $a = 0.05$ and $M_0 = 340 \text{ MeV}$.

(weak first-order), and (3) $b = 0.08M_0^3$ and $g_v = 0.12/M_0^2$ (crossover).

For later convenience we shall plot the energy per particle ε/ρ_B at $T = 0$ in Fig. 3, where $\varepsilon = \Omega/V + \mu_B \rho_B - \Omega_0/V$ is the internal energy density measured from the hadronic vacuum with $M \sim M_0$, and $\rho_B = \rho/N_c$ is the baryon number density. If the curve has a minimum as a function of ρ_B , i.e. $d(\varepsilon/\rho_B)/d\rho_B = \mu_B/\rho_B - \varepsilon/\rho_B^2 = 0$, the pressure difference becomes zero, which indicates a first-order phase transition of the general liquid-gas type (see Ref. [20] for a nice review). Therefore, whenever ε/ρ_B has a minimum as a function of ρ_B , the $T = 0$ system must have a first-order phase transition in the same way as the nuclear matter phase transition at $\mu_B = M_N - B$ with M_N being the nucleon mass and B the nuclear binding energy. At the second-order transition, the energy curve should be flat at the point of inflexion. This kind of analysis on quark matter is well known in the context of quark droplets [21] but less applied in the phase diagram research. What is necessary for the existence of the critical point (first-order phase transition) is a convex structure of the curve (saturation property), which is a general statement that does not rely on any model nor Ansatz.

Because this point of the liquid-gas transition is so important, let us recall here how an intermediate density between zero and the saturation density ρ_0 can be realized in this case. As schematically shown in Fig. 4 it would be energetically preferable to form bubbles with ρ_0 . If we consider the surface energy, the density gradient (Weizsäcker) term, and the charge neutrality, bubbles should take the optimal shapes such as the nuclear pasta [22]. This state of matter is nothing but a mixed phase associated with the first-order phase transition, and importantly, this argument already implies an inhomogeneous ground state near the liquid-gas transition. In other words, if a mixed phase is characterized by a

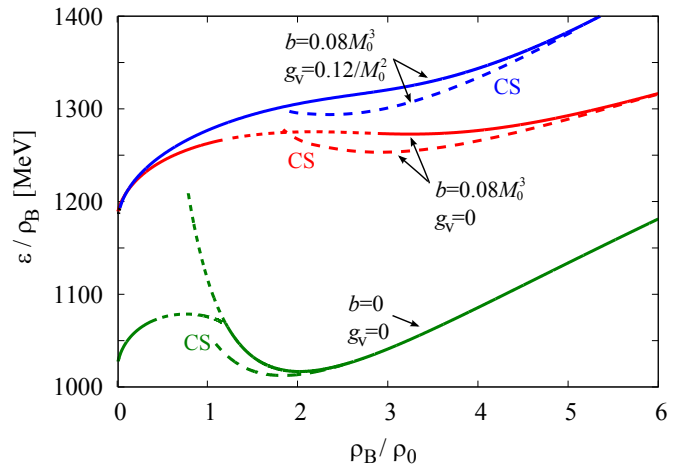


FIG. 3. Energy per particle as a function of the density. The solid curves represent the homogeneous results for (1) $b = g_v = 0$, (2) $b = 0.08M_0^3$ and $g_v = 0$, (3) $b = 0.08M_0^3$ and $g_v = 0.12/M_0^2$ from the bottom to the top. The dashed curves with the label “CS” represent the chiral-spiral results for respective parameters. The horizontal axis is given in the unit of the normal nuclear density $\rho_0 = 0.17 \text{ fm}^{-3}$.

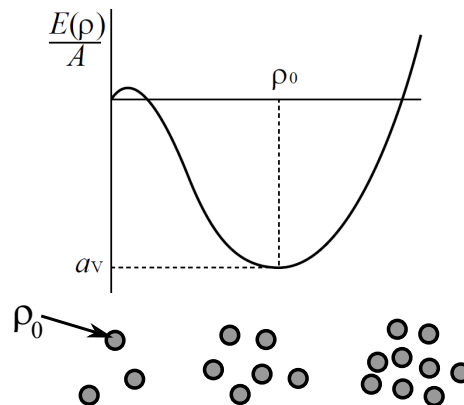


FIG. 4. Schematic figure of the saturation curve of nuclear matter with a minimum at $\rho_0 = 0.17 \text{ fm}^{-3}$ and the binding energy given by the volume term a_V in the Bethe-Weizsäcker mass formula. An intermediate density $\rho < \rho_0$ can be realized by bubbles with ρ_0 in the empty whose shapes would depend on the surface term a_S , etc.

typical wave number q , how can we distinguish such a phase from an inhomogeneous ground state? One may think that in the case of quark matter the inhomogeneity is turned on not in the density only but in the mass M unlike nuclear matter. We would stress, however, that M also controls the density and the physics is just the same if seen on the saturation curve as in Fig. 3.

It is obvious from Fig. 3 that the vector interaction as in Eq. (3) disfavors the first-order phase transition. The minimum in ε/ρ_B is pushed up by the quadratic term and eventually the first-order phase transition disappears when the minimum is lost, as demonstrated by three solid curves in Fig. 3. In the chiral limit $b = 0$

the branch of $M = 0$ is separate, so that the first-order phase transition survives regardless of the vector interaction. With finite b , however, two branches with small and large M are smoothly connected and the minimum diminishes for large b and g_v in accord to Fig. 2.

One may find its usefulness for analyses with a wider range of model space. From now on we shall consider the possibility to form inhomogeneous chiral condensates. We here utilize the simplest Ansatz to introduce it, namely, the one-dimensional chiral spiral; $\langle \bar{\psi}\psi \rangle = \chi \cos(2qz)$ and $\langle \bar{\psi}\gamma_5\tau_3\psi \rangle = \chi \sin(2qz)$ [23]. This ground state of the chiral spiral can be equivalently described by a chiral rotation $\psi = e^{i\gamma_5\tau_3qz}\psi'$ with a homogeneous condensate $\chi = \langle \bar{\psi}'\psi' \rangle$ in the chiral limit. Then, the quasi-particle dispersion relation in the ψ' -basis is expressed as

$$\tilde{\omega}_p = \sqrt{p_\perp^2 + (\sqrt{p_z^2 + M^2} \pm q)^2}, \quad (4)$$

where \pm in front of q corresponds to the flavor and the chirality that also depends on the sign of p_z .

This dispersion relation (4) should be plugged into Ω_{matter}/V in Eq. (1). Unlike the normal dispersion relation, we see that a large part of the mass effect can be absorbed by $q \sim M$, with which ρ is no longer suppressed even at large M . This is the reason why a first-order phase transition occurs from the homogeneous hadronic phase to the chiral spiral where M is substantially large. Also, we should point out that the Ginzburg-Landau analysis in Ref. [25] to conclude that the chiral spiral is less favored is insufficient. The largest energy gain in Ω_{matter}/V comes from the region where the Ginzburg-Landau expansion does not work. Thus, it is Ω_0/V that would hinder the growth of q . In the leading order the vacuum part has an expansion in terms of q as

$$\Omega_0[M, q]/V = \Omega_0[M]/V + (\alpha M^2 + \beta b)q^2, \quad (5)$$

where the first term with $\alpha > 0$ is a ‘‘kinetic’’ term against spatial modulation. This term should be vanishing at either $M = 0$ or $q = 0$, so the expansion should start with M^2q^2 . One can estimate α using a chiral model, but one should be careful not to pick an unphysical term $\sim \Lambda^2q^2$ up from gauge-variant regularization. The latter term $\propto \beta$ comes from a phase of the current mass term associated with the basis change from ψ to ψ' . Quantitative details may depend on α and β , but qualitative features as we discuss below do not refer to any specific choice of them.

Figure 5 shows typical behavior of the phase boundary on the μ_q - T plane with zero and non-zero b and g_v . For demonstration we chose $\alpha = 0.25$ and $\beta = 0.25/M_0$. Then in the lower- μ_q side of Fig. 5 we see that there is an island structure of the chiral spiral surrounded by the first-order boundaries. The dashed curve represents a first-order phase transition with the homogeneous condensate only. The first-order boundary of inhomogeneity at smaller μ_q stays very close to the dashed curve. This is because the potential depth becomes very shallow

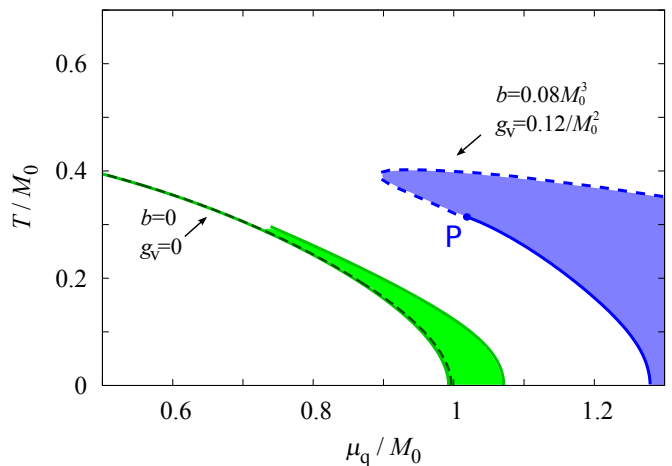


FIG. 5. Typical phase diagrams with the chiral spiral for zero and non-zero b and g_v . The inhomogeneous region is enlarged with $b = 0.08M_0^3$ and $g_v = 0.12/M_0^2$ with which the homogeneous transition would be crossover entirely but the inhomogeneous one still forms a rich structure.

near the first-order phase transition in the homogeneous case as clearly recognized in the total potential in Fig. 1. The secondary first-order boundary at larger μ_q is much weaker because M and thus q are small there. The corresponding saturation curve of ε/ρ_B is shown by a long-dashed curve with the label ‘‘CS’’ in Fig. 3, from which a minimum at lower energy is apparent. We note that the inhomogeneity island in the vicinity of the first-order phase transition is consistent with our intuitive picture of the mix phase formation.

With the vector interaction included, the so-called QCD critical point is easily washed out. Interestingly, however, as shown in the higher- μ_q side of Fig. 5 and especially P in this figure, there is a chance that the critical point (strictly speaking, tri-critical point) is revived driven by the inhomogeneous condensate. The question is then how robust this observation is. In fact it has been reported that the soliton solution [24] is more stable than the chiral spiral and also it exhibits a second-order phase transition [25].

Let us then consider when the second-order phase transition is possible in view of the saturation curve in Fig. 3. To have a second-order phase transition from the hadronic phase (with homogeneous $M \sim M_0$) to a general inhomogeneous state, there must be an energy curve that is tangent to the hadronic branch (solid curves from $\rho_B = 0$) and goes below it. The curves does not have to be flat because there is a small energy difference before and after a finite density appears, which is further enhanced by $1/\rho_B^2$ in the slope of the saturation curve. To avoid a first-order transition, moreover, the energy curve should be monotonically increasing with increasing ρ_B .

Such a situation is not allowed, for example, in the far bottom curves in Fig. 3. In this case with the saturation energy as low as that at ρ_B , we can conclude that only a first-order phase transition is possible however compli-

cated and optimized modulations we introduce. Also, it is clear that a larger g_v would ease better inhomogeneous states to develop, for the dashed chiral-spiral curve could be easily extended down to $\rho_B = 0$ monotonically. Therefore, unfortunately, the existence of the critical point P is again not a robust conclusion especially with the vector interaction.

From a plain physical interpretation, it would be the most natural to have second-order phase transitions that border the inhomogeneous island. Such an intuition is based on the picture of the liquid-gas phase transition. In fact, if the boundary is a first-order phase transition, there will appear a density regime that can be described only as a mixed state. It is the chiral condensate in quark matter that makes a sharp contrast to the situation in nuclear matter. The density modulation in a mixed state can be mimicked by the modulation in the chiral condensate, which would lead to an inhomogeneous ground state of quark matter with lower energy. This is exactly what is happening in the soliton solution in Refs. [24, 25]. Indeed, at the onset of soliton inhomogeneity, a localized domain-walls start appearing, which approaches sinusoidal patterns at larger μ_q . The density profile has peaks arising

from the solitons and this situation is reminiscent of a mixed state picture as schematically depicted in the bottom of Fig. 4. It would be interesting to figure out the saturation curve corresponding to the soliton solution.

In summary, we have developed a picture of the first-order phase transition of quark matter based on the saturation curve and the liquid-gas phase transition. From this picture we discuss the relation between the order of the phase transition and the behavior of the saturation curve. We demonstrated this using a simple Ansatz of the chiral spiral, but the argument itself is not limited to such a special choice. Actually, because the chiral spiral can be mapped to the conventional pion condensation [26] that is killed by the spin-isospin interaction, it is likely that the chiral spiral should be disfavored by the axial-vector interaction $\sim (\bar{\psi}\gamma_5\gamma_\mu\psi)^2$ or $\sim (\bar{\psi}\gamma_5\gamma_\mu\vec{\tau}\psi)^2$, and eventually superseded by others such as the soliton-like modulation and more generally multiple-wave superpositions. It may be interesting to seek for some connections between our saturation considerations and the Ginzburg-Landau analyses as in Ref. [27].

The author thanks Tetsuo Hatsuda, Yoshimasa Hidaka, Larry McLerran, Wolfram Weise for critical comments and useful discussions.

-
- [1] M. G. Alford, A. Schmitt, K. Rajagopal and T. Schafer, *Rev. Mod. Phys.* **80**, 1455 (2008).
- [2] L. McLerran and R. D. Pisarski, *Nucl. Phys. A* **796**, 83 (2007); T. Kojo, Y. Hidaka, K. Fukushima, L. McLerran and R. D. Pisarski, *Nucl. Phys. A* **875**, 94 (2012).
- [3] A. Andronic, D. Blaschke, P. Braun-Munzinger, J. Cleymans, K. Fukushima, L. D. McLerran, H. Oeschler and R. D. Pisarski *et al.*, *Nucl. Phys. A* **837**, 65 (2010).
- [4] M. Asakawa and K. Yazaki, *Nucl. Phys. A* **504**, 668 (1989); A. Barducci, R. Casalbuoni, S. De Curtis, R. Gatto and G. Pettini, *Phys. Lett. B* **231**, 463 (1989); A. Barducci, R. Casalbuoni, G. Pettini and R. Gatto, *Phys. Rev. D* **49**, 426 (1994).
- [5] H. Meyer-Ortmanns, *Rev. Mod. Phys.* **68**, 473 (1996); V. I. Yukalov and E. P. Yukalova, *Phys. Part. Nucl.* **28**, 37 (1997); D. H. Rischke, *Prog. Part. Nucl. Phys.* **52**, 197 (2004).
- [6] K. Fukushima and T. Hatsuda, *Rept. Prog. Phys.* **74**, 014001 (2011); K. Fukushima, *J. Phys. G* **39**, 013101 (2012).
- [7] F. Becattini, J. Manninen and M. Gazdzicki, *Phys. Rev. C* **73**, 044905 (2006); A. Andronic, P. Braun-Munzinger and J. Stachel, *Phys. Lett. B* **673**, 142 (2009).
- [8] K. Fukushima, *Phys. Lett. B* **695**, 387 (2011).
- [9] J. Cleymans, H. Oeschler, K. Redlich and S. Wheaton, *Phys. Rev. C* **73**, 034905 (2006).
- [10] S. Floerchinger and C. Wetterich, arXiv:1202.1671 [nucl-th].
- [11] M. A. Stephanov, K. Rajagopal and E. V. Shuryak, *Phys. Rev. Lett.* **81**, 4816 (1998); *Phys. Rev. D* **60**, 114028 (1999); M. A. Stephanov, *Phys. Rev. Lett.* **102**, 032301 (2009).
- [12] G. Endrodi, Z. Fodor, S. D. Katz and K. K. Szabo, *PoS LAT 2007*, 182 (2007); J. -W. Chen, K. Fukushima, H. Kohyama, K. Ohnishi and U. Raha, *Phys. Rev. D* **81**, 071501 (2010).
- [13] J. Braun, L. M. Haas, F. Marhauser and J. M. Pawłowski, *Phys. Rev. Lett.* **106**, 022002 (2011); C. S. Fischer, *Phys. Rev. Lett.* **103**, 052003 (2009).
- [14] C. Ratti, M. A. Thaler and W. Weise, *Phys. Rev. D* **73**, 014019 (2006); M. Ciminale, R. Gatto, N. D. Ippolito, G. Nardulli and M. Ruggieri, *Phys. Rev. D* **77**, 054023 (2008); W. j. Fu, Z. Zhang and Y. x. Liu, *Phys. Rev. D* **77**, 014006 (2008); K. Fukushima, *Phys. Rev. D* **77**, 114028 (2008); T. K. Herbst, J. M. Pawłowski and B. -J. Schaefer, *Phys. Lett. B* **696**, 58 (2011); B. J. Schaefer and M. Wagner, *Phys. Rev. D* **85**, 034027 (2012).
- [15] R. D. Pisarski and F. Wilczek, *Phys. Rev. D* **29**, 338 (1984).
- [16] T. Hatsuda, M. Tachibana, N. Yamamoto and G. Baym, *Phys. Rev. Lett.* **97**, 122001 (2006).
- [17] K. Fukushima, *Phys. Rev. D* **78**, 114019 (2008).
- [18] T. Hatsuda and T. Kunihiro, *Phys. Rept.* **247**, 221 (1994).
- [19] S. Klimt, M. Lutz and W. Weise, *Phys. Lett. B* **249**, 386 (1990); *Nucl. Phys. A* **542**, 521 (1992).
- [20] P. Chomaz, nucl-ex/0410024.
- [21] M. Buballa, *Nucl. Phys. A* **611**, 393 (1996); M. Buballa and M. Oertel, *Nucl. Phys. A* **642**, 39 (1998).
- [22] G. Watanabe, K. Iida and K. Sato, *Nucl. Phys. A* **676**, 455 (2000).
- [23] V. Schon and M. Thies, In *Shifman, M. (ed.): At the frontier of particle physics, vol. 3* 1945-2032; E. Nakano and T. Tatsumi, *Phys. Rev. D* **71**, 114006 (2005).
- [24] D. Nickel, *Phys. Rev. D* **80**, 074025 (2009).
- [25] S. Carignano, D. Nickel and M. Buballa, *Phys. Rev. D*

- 82**, 054009 (2010).
- [26] A. B. Migdal, *Rev. Mod. Phys.* **50**, 107 (1978).
- [27] H. Abuki, D. Ishibashi and K. Suzuki, arXiv:1109.1615 [hep-ph].